



# Size-dependent thermal properties of multi-walled carbon nanotubes embedded in phase change materials

Umit Nazli Temel<sup>1</sup> · Sengul Kurtulus<sup>1</sup> · Murat Parlak<sup>2</sup> · Kerim Yapici<sup>3</sup>

Received: 1 August 2017 / Accepted: 5 January 2018 / Published online: 18 January 2018  
© Akadémiai Kiadó, Budapest, Hungary 2018

## Abstract

This study has focused on the systematical investigation of effect of mass fraction and size of multi-walled carbon nanotubes (MWCNTs) doped in phase change material (PCM) on thermal properties such as thermal conductivity, melting/solidification temperatures and latent heats. Thermal conductivity, melting/solidification temperatures and latent heats of MWCNTs/PCM composites with three different diameters and two different lengths, obtained by doping MWCNTs into PCM at the mass fraction of 1–5%, were evaluated according to the criteria such as particle size and mass fraction. The results demonstrated that not only mass fractions but also size of MWCNTs are effective on the thermal properties of the composites. It was concluded that increase in diameter and length of MWCNTs positively affects enhancement of thermal conductivity; on the other hand, it does not cause a significant change at melting/solidification temperatures. In addition to these, a decline was observed at melting/solidification latent heats of MWCNTs/PCM composites, depending on doped mass fractions of MWCNTs.

**Keywords** Thermal conductivity · Multi-walled carbon nanotubes (MWCNTs) · Phase change materials (PCMs) · Size dependency

## Introduction

Decreasing the consumption of fossil fuel due to its adverse affects on environmental pollution and climate change pointed the attention to renewable energy sources. The intermittent nature of renewable energy sources such as sun and wind in regard to time and weather conditions and incompatibilities between energy conversion time and energy utilization require the development of efficient energy storage systems. Similarly, the regaining of waste heat released from the widely used thermal energy conversion systems such as power plants and motors increases the efforts for energy storage. Phase change materials (PCMs) are energy storage materials with high latent heat,

having ability to transform from solid to liquid or from liquid to solid, showing low-temperature change [1]. The PCMs due to having high energy storage capability have been widely used in many fields of engineering such as energy storage [2], active and passive cooling [3, 4], thermal protection of electronic devices operating temporarily [5, 6]. PCMs application is generally focused to increase system performance. For example, Weng et al. [7] determined that fan power consumption of a heating pipe used for electronic cooling purposes diminished by 46% when used together with an energy storage unit containing PCM as opposed to a traditional heating pipe. Zhou et al. [8] put forth that using PCM instead of sand as thermal storage material in a low-temperature floor heating system causes the more uniform heating (< 0.3 °C). Additionally, they showed that heat propagation time of the PCM used system two times more than that of the sand used system when the heat source was closed. In another study, Barzin et al. [9] measured that there would be a 73% weekly gain in terms of energy saving, when the PCM incorporated into plasterwork is used for passive cooling purposes in buildings. Recently, Jin et al. [10] determined

✉ Kerim Yapici  
kerim yapici@sdu.edu.tr

<sup>1</sup> Department of Energy Systems Engineering, Cumhuriyet University, 58140 Sivas, Turkey

<sup>2</sup> Aselsan Inc Rehis-Energy Division, 06830 Ankara, Turkey

<sup>3</sup> Department of Chemical Engineering, Suleyman Demirel University, 32260 Isparta, Turkey

optimal phase change temperature range and optimal PCM location in the building wall during different seasons under weather conditions. Ye [11] examined the effects of the fins number and outer wall boundary conditions on the energy storage capacity of a double tube that contains commercial PCM. It is found that the melting rates increase as the fins number increases. Hadiya et al. [12] investigated experimental performance of paraffin wax using shell and tube heat exchanger during energy charging and discharging cycle under different flow rates. They determined that charging and discharging time decreases with increase in mass flow rate of heat transfer fluid and fall in the time during discharge is around three times faster than charging.

PCMs are divided into three categories including organic (paraffins), inorganic (hydrate salts) and eutectoid. Organic PCMs from phase change materials are the most preferred and used type of material because of having some advantages such as high latent energy and low vapor pressure, chemical and thermal stability, no subcooling property during solidification process and easily and economically attainable [13, 14]. On the other hand, a well-known serious disadvantage of organic phase change materials is having very low thermal conductivity. This case significantly slows down the speeds of heat charge/discharge of organic PCMs. The low thermal conductivity of organic PCMs should be improved in order that they can be used effectively. On the other hand, thermal properties such as melting/solidification latent heats and temperatures are not to be deteriorated while improving thermal conductivity. In order to solve this problem, several methods such as inserting high conductivity metal fins [15, 16], foams [17] and matrices [18] into PCM have been implemented from past to present. Yang et al. compared the dynamic thermal behavior of a shell and tube energy storage unit for the PCM and the PCM/Cu foam composite. They showed the meltdown period of the PCM/Cu foam composite to be 33% as shorter under identical experimental conditions [19]. Although these methods improve thermal conductivities of PCMs, they cause several disadvantages such as increase in system weight and/or volume, poor stability [20], crystallization problems, reduction in the amount of PCM used. Over the last decade, development of nanotechnology enables the synthesis of nano-sized particles in different types and sizes (< 100 nm) which led to the development of a more innovative method for enhancement of the thermal conductivities of the organic PCMs [21]. This method is based on creation of a new nanoparticle/PCM composite by doping metal/metal oxide or carbon-based nanoparticles into organic PCM at a certain mass ratio. The studies revealed that multi-walled carbon nanotubes (MWCNTs) can be used as a suitable additive materials for enhancement of thermal conductivity of PCMs because of having high thermal

conductivity and light weight. On the other hand, failure of obtaining homogeneous dispersion and keeping stability particularly in high doping mass fractions through long terms are major challenges.

Several studies have been carried out in the literature to investigate effect of the loading of MWCNTs into the PCMs for enhancement of the thermal properties of MWCNTs/PCM composites. It was determined that thermal conductivity increases depending on the mass fraction of MWCNTs [22–24]. In addition to this, it was reported that the increase in thermal conductivity was in the range of 24–30% in the case of 5% mass fraction, depending on the size of MWCNTs doped into the PCM [25, 26]. On the other hand, it was revealed that enhancement of thermal conductivity can be risen up to the level of 50% as a result of being functionalized of MWCNTs or physical (ball milling) pretreatments [27]. It was reported that since surface area of MWCNTs is increased by connecting some functional groups such as hydroxyl, carboxylic and amidocyanogen to its surface during these pretreatments [28], it shows better performance in enhancement of thermal conductivity as compared to pristine MWCNTs.

Despite the increase in its thermal conductivity, there is conflicting information in the literature regarding change of other thermal properties such as melting/solidification temperatures and melting/solidification latent heats depending on amount, size and functional groups of MWCNTs doped. There are studies reporting that heat storage capacity decreases [25, 29], increases [30] or does not change [31] depending on the doped mass fractions of nanoparticles. Heat storage capacity depends strongly on the sample mass. It has been considered that in this case, some weighing errors could have been made during preparation of samples for differential scanning calorimeter (DSC) measurements. DSC manufacturers recommend samples to be prepared by using balances with precision of at least 0.01 mg. It was also reported in the literature that thermal properties of composites improved strongly depend on size and shape of nanoparticles. These studies have been usually concentrated on the shape effect and include comparisons of thermal properties of wire and planar-shaped nanoparticles [29, 30].

As it can be seen from the above brief literature survey, the number of studies investigating size effect of MWCNTs used on thermal properties of MWCNTs/PCM composite obtained is highly limited. Therefore, this study aims to systematically investigate the size effect of nanoparticles on thermal properties of MWCNTs/PCM composites. As listed in Table 1, MWCNTs used in this study were selected in three different diameters and in two different lengths for each diameter. The systematic comparison of thermal properties of MWCNTs/PCM composites was performed at 1, 3 and 5% mass fractions for each

**Table 1** Properties of MWCNTs

Nanomaterial type	Length/ $\mu\text{m}$	Outer/inner diameter/nm	Surface area/ $\text{m}^2\text{g}^{-1}$
Long (L-MWCNTs)	10–30	< 7/2–5	> 500
Long (L-MWCNTs)	10–30	20–30/5–10	> 110
Long (L-MWCNTs)	10–30	50–80/5–15	> 40
Short (S-MWCNTs)	0.5–2	< 7/2–5	> 500
Short (S-MWCNTs)	0.5–2	20–30/5–10	> 110
Short (S-MWCNTs)	0.5–2	50–80/5–15	> 40

type of MWCNTs. Another objective of this study is determination of the change in thermal properties of the composite depending on mass fractions of MWCNTs. In the light of the results obtained, conflicting information in the literature is attempted to be made clear.

## Experimental method

Paraffin wax organic PCM, the melting temperature of which is about 343 K, was commercially supplied from Phase Change Material Products Limited (UK) and used in all experiments without any pretreatment. One of the most important applications of PCM is thermal protecting of the electronic devices. For the many electronic devices, thermal protecting temperature limit is about 358 K. Therefore, in this study, PCM with a melting temperature of 343 K was selected. MWCNTs selected in three different diameters and two different lengths for each diameter were commercially supplied from US Research Nanomaterials Inc (USA) and used without any pretreatment. Nanomaterials with length ranging between 0.5 and 2  $\mu\text{m}$  are called as short (S-MWCNTs), those with length ranging between 10 and 30  $\mu\text{m}$  are called as long (L-MWCNTs). The purity of all MWCNTs is more than 95%, and its other properties are listed in Table 1.

MWCNTs/PCM composites were prepared by applying two steps melting–mixing procedure. In the first step, as seen in Fig. 1a, PCM was melted by heating on a hot plate. Afterward, MWCNTs were added into liquid PCM at the mass fractions of 1, 3 and 5% (Fig. 1b). In the second step, in order to provide uniform dispersion of MWCNTs into liquid PCM, stirring process was carried out by using an 750 W ultrasonic stirrer (Sonics and Materials INC, USA) for 30 min (Fig. 1c). The temperature was kept above PCM melting temperature in order prevent composite to solidify during stirring process.

In order to see the dispersion of MWCNTs within the PCM matrix, the SEM (Tescan Mira 3 XMU, Czechia) images of the composite that doped with 3% S-MWCNTs with a diameter of 20–30 nm are given in Fig. 2. The average size of the MWCNTs is determined as about 90 nm within the PCM matrix. This shows that MWCNTs

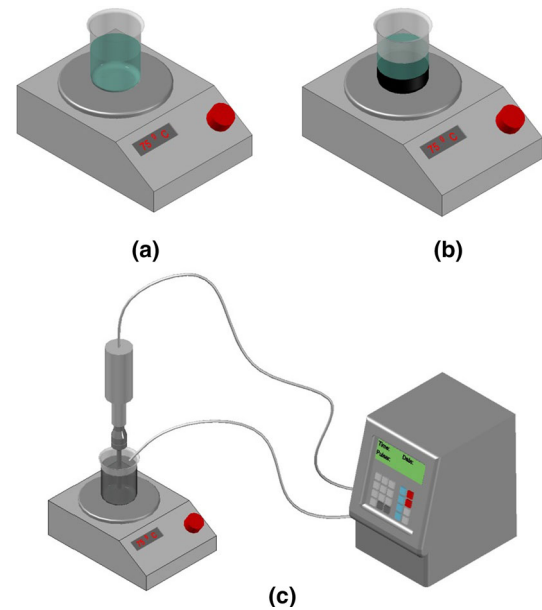


**Fig. 1** Schematic representation of preparation of MWCNTs/PCM composites

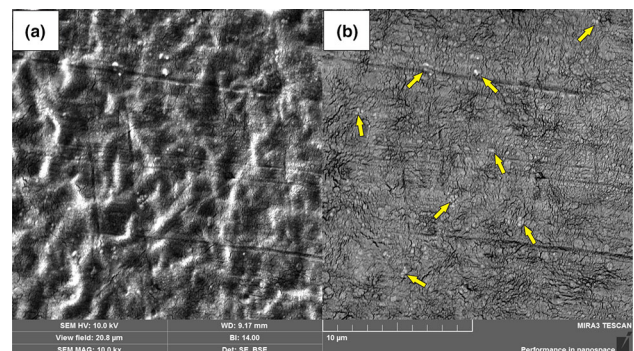


**Fig. 2** SEM images a) the secondary electron imaging, b) the backscattered electron imaging

are exposed to slight agglomeration due to mixing process. The secondary electron imaging (Fig. 2a) shows homogeneous distribution of MWCNTs within the PCM matrix. It also shows that neither the MWCNTs are pulled nor the PCM shows any incompatibility in the composite. The

MWCNTs are heavier elements ( $2.1 \text{ g cm}^{-3}$ ) which backscatter more efficiently and appear brighter than lighter PCM ( $0.9 \text{ g cm}^{-3}$ ) in a backscattered electron image (Fig. 2b). Backscattered electron imaging shows the MWCNTs are separated individually in PCM matrix.

In order to obtain measurement samples, liquid MWCNTs/PCM composite was poured into the acrylic cylindrical mold with 30 mm in diameter and 150 mm high and provided being solidified. Thermal conductivity measurements of MWCNTs/PCM composites were taken by using KD2 Pro device (Decagon Devices Inc., USA) operating on the basis of temporary linear heat source. Briefly, KD2 Pro device consists of a microcontroller and a sensor needle of 100 mm long and 2.4 mm diameter. High L/D ratio provides elimination of end effects. The sensor needle works both as a heater and temperature sensor and determines the temperature change during passage of current throughout heater for a time period. Thermal conductivity has been determined as a result of analysis of the measured temperature for a time period. In order to perform the measurements, a hole in appropriate size for sensor needle was made in the center of the sample. According to manufacturer's recommendations, the TR1 sensor was used for the measurements of solid composite samples. Before starting the measurements, the accuracy of KD2 Pro device was confirmed by measuring the thermal conductivity of known solid sample. The measurements of all samples were performed at 303 K. At least six measurements were taken for each sample, and the mean values with standard deviation of 0.5% are given as the result. The accuracy of the measurements is  $\pm 5\%$  for the range of  $0.2\text{--}2 \text{ W m}^{-1} \text{ K}^{-1}$  and  $\pm 0.02 \text{ W m}^{-1} \text{ K}^{-1}$  for the range of  $0.1\text{--}0.2 \text{ W m}^{-1} \text{ K}^{-1}$ .

Other thermal properties including melting/solidification temperatures and latent heats were measured by using differential scanning calorimetry (Shimadzu Corporation, Japan). The samples for DSC analysis were prepared by weighing in the range of 4–6 mg in an aluminum pan by using electronic balance with precision of 0.01 mg (Shimadzu Corporation, Japan). The calibration of the DSC device was performed using standard sample of indium before starting the measurement. The measurements with DSC device were taken at  $2 \text{ K min}^{-1}$  heating/cooling rate and in the range of 303–433 K. The analysis of DSC curves may change depending on the person determining the tangent points on the curve to perform the analysis. It is more appropriate to carry out more than one analysis at different times to give the results as the average of these measurements. In this work, the measurements were taken at least three times for each sample and the mean values with standard deviations of 1% are given as the result. The precision and accuracy of the DSC device are, respectively,  $\pm 0.1\%$  and  $\pm 0.1 \text{ K}$ .

## Results and discussion

In this section the thermal conductivity values and DSC results of MWCNTs/PCM composites are given and discussed in detail. The variation of the thermal conductivities of S-MWCNTs/PCM and L-MWCNTs/PCM composites with respect to mass fractions of MWCNTs is given in Fig. 3. It should firstly be noted that thermal conductivity of PCM was measured as  $0.402 \text{ W m}^{-1} \text{ K}^{-1}$ . It was concluded through detailed analysis of the results given in Fig. 3 that (1) at low MWCNTs mass fractions (1 wt%), thermal conductivity of PCM composites doped with S-MWCNTs with three different diameters was less than that of PCM. Similar results were reported in the study performed by Zeng et al. [23] in which the thermal properties of PCM composites doped with MWCNTs were investigated. In their experimental study, Zeng et al. (2009) emphasized that thermal conductivity value of the composite doped with MWCNTs at low mass fractions is deteriorated as compared to undoped PCM. It has been explained that main obstacle to use MWCNTs as thermal enhancer filler is its high interface thermal resistivity [32]. In addition to this, failure of creating continuous and effective network structure in low mass fractions is the main reason for deterioration in thermal conductivity. In the absence of effective heat conduction network, the high thermal resistivity between MWCNTs and PCM matrix would cause decrease in thermal conductivity. While deterioration of thermal conductivity for the composite doped with 1% mass fraction of S-MWCNTs with  $< 7 \text{ nm}$  outer diameter was measured as 2.74%, it was measured, respectively, as 4.48 and 3.73% for S-MWCNTs with 20–30 nm and 50–80 nm outer diameter, respectively. However, thermal conductivity value increases due to the formation of effective conduction network structure after mass fraction of MWCNTs has reached to a certain value. Heat transfer by conduction is achieved by phonon transfer, which is related to the size of the nanomaterial lattice and the frequency of the vibration [33]. In addition, the thermal conductivities of PCMs are low due to both low frequency of vibration and the inhibition of phonon transfer. In contrast, doping MWCNTs which have high vibration frequency into PCMs leads to improved phonon dispersion and therefore resulting in increased heat conduction. As a result, it can be said that this significant improvement in thermal conductivity is related to the formation of a suitable MWCNTs network for phonon dispersion. At this point enhancement in thermal conductivity due to effective phonon transfer through network compensates the deterioration due to high thermal resistivity between MWCNTs and PCM interface. (2) For each type of MWCNTs, a nonlinear increase was observed in thermal conductivity

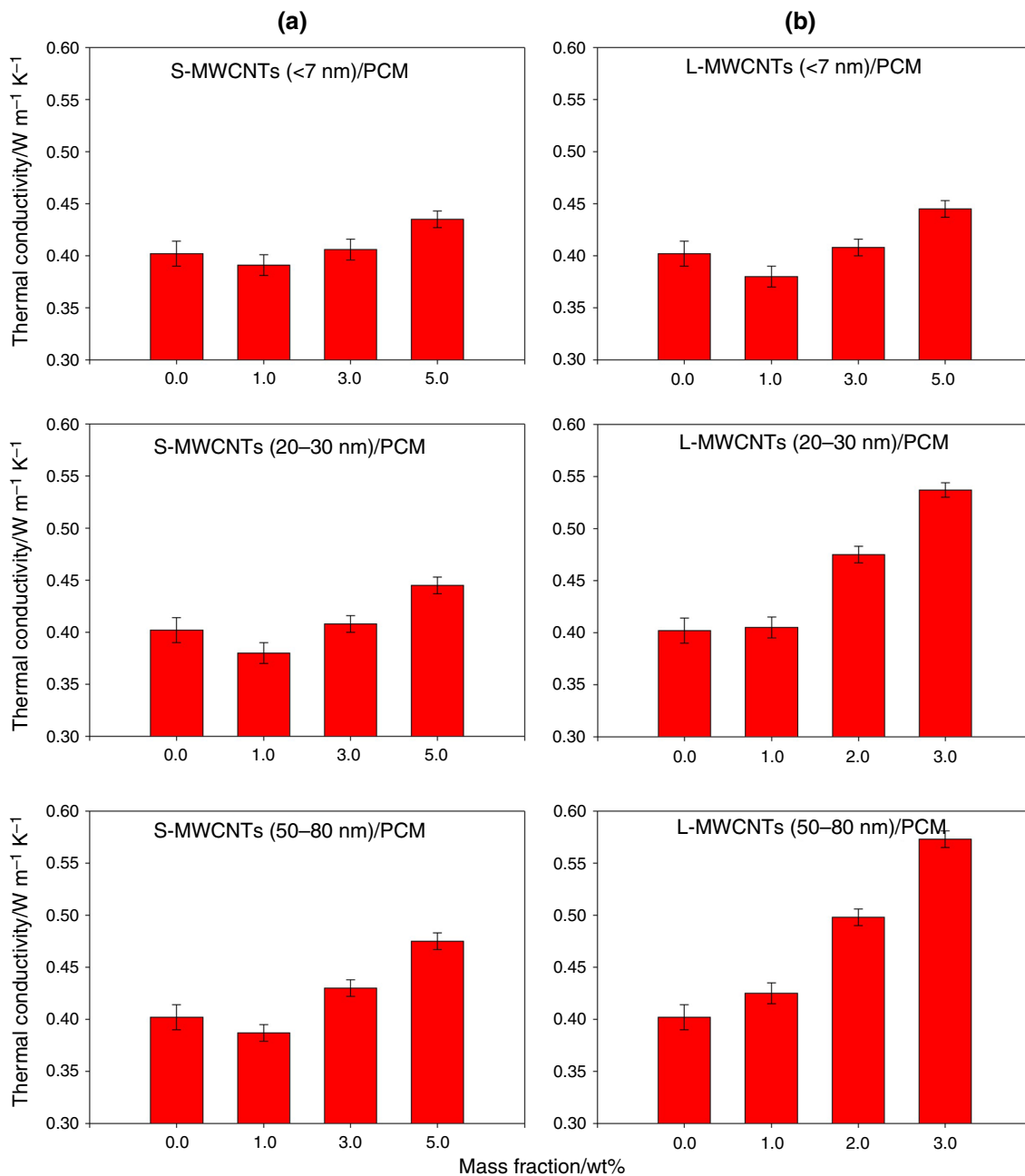


**Fig. 3** Variation of thermal conductivity of S-MWCNTs/PCM and L-MWCNTs/PCM composites as function of mass fractions

depending on the increase in the mass fraction of MWCNTs. (3) It was observed that enhancement of thermal conductivity changes depending on the outer diameter of MWCNTs doped. This can be more strongly seen in the PCM composites doped especially with L-MWCNTs. For example, enhancement of thermal conductivity of PCM composites doped with 5% mass fractions of L-MWCNTs with outer diameters of < 7 nm, 20–30 nm and 50–80 nm was measured as 9.95, 33.60 and 42.54%, respectively. The results showed that positive effect of MWCNTs diameter on effective phonon transports within the composites.

Increase in the diameter of MWCNTs within the PCM improves the phonon transfer, and therefore it enhances the thermal conductivity. (4) The enhancement of the thermal conductivity of composites doped with L-MWCNTs resulted higher than that of composites doped with S-MWCNTs depending on the mass fractions. For example, while the enhancement of thermal conductivity of composite doped with 5% mass fraction of S-MWCNTs with an outer diameter of 50–80 nm was determined as 18.41%, the enhancement of thermal conductivity of composite doped with L-MWCNTs with the same outer



diameter and mass fraction was determined as 42.54%. It was considered that obtaining a higher enhancement in the value of thermal conductivity when L-MWCNTs is used is associated with decrease in tube–tube and tube–PCM interface resistances and eventually creation of more efficient network structure.

The organic PCMs possess a good long-term thermal stability and chemical reliability in terms of melting temperature and latent heat of fusion [34]. Preparing a thermally stable nanoparticle/PCM composite is undoubtedly the first and foremost important step in the research and application of PCM composites. Here the thermal stability of MWCNTs/PCM composites was analyzed by measuring their thermal conductivity at various heating–cooling cycles. Figure 4 depicts the variation of thermal conductivity with respect to twenty heating–cooling cycles for MWCNTs/PCM composite doped with 5% mass fraction of L-MWCNTs with 50–80 nm outer diameters. At the end of five cycles, 4.8% decrease in thermal conductivity was observed. Between five and twenty heating/cooling cycles, the thermal conductivity appears to be almost constant. During the twenty heating/cooling cycles, decrease in thermal conductivity is less than 6.1%. If the total enhancement in thermal conductivity is considered, it can be said that the deterioration observed in thermal conductivity during twenty heating/cooling cycles may be neglected.

The thermal performances of the composites which have been obtained by being doped with single- and multi-walled CNTs until today are given in Table 2 in detail. When the results given in Table 2 are reviewed, it can be seen that the rate of increase in thermal conductivity ranges between 24 and 51.6% in the highest mass CNTs fraction. In some of the studies listed in Table 2 [16, 22, 23], thermal conductivity enhancement up to 50% was obtained at lower mass fractions as a result of subjecting MWCNTs to

pretreatments physically and chemically before being doped into PCM. On the other hand, different rates of increase in thermal conductivity were obtained for the same MWCNTs mass fraction in other studies other than those mentioned. It is considered that this situation is associated with size of MWCNTs used and the process applied in composite preparation.

A brief review of the literature and the results revealed that enhancement of thermal conductivity of MWCNTs/PCM composites was quite low, although thermal conductivity value of MWCNTs was quite high ( $< 3000 \text{ W m}^{-1} \text{ K}^{-1}$ ). In their experimental study, Wang et al. [23] suggested that low enhancement of thermal conductivity observed in MWCNTs/PCM composites could be resulted from (1) scattering of heat carrying phonon on the CNTs and PCM interface and (2) high thermal resistance on CNTs surfaces doped inside PCM. In addition to these, it can arise from unrevealing of effective thermal conductivities of MWCNTs in the matrix by being encapsulated by PCM.

DSC analyses were performed to investigate the effects of mass fractions of MWCNTs on melting/solidification temperatures and latent heats. DSC curves involving heating/cooling cycles of the composites obtained through all MWCNTs are given in Fig. 5. As it can be seen from the figure that DSC curves of all MWCNTs/PCM composites are similar to that of the PCM. The endotherm and exotherm peaks occurred in the DSC curves during heating and cooling indicate that phase change occurs in a wide temperature range. In addition to this, it was determined that endotherm/exotherm peak amplitude decreases depending on the amount of MWCNTs doped and increases depending on the amount of the sample prepared. The areas under the endotherm and exotherm peaks give latent heat values for melting and solidification, respectively. The variation of the endotherm and exotherm peaks amplitude is an indication of the change in latent heats. On the other hand, it was determined that the decrease in the endotherm/exotherm peak amplitudes of S-MWCNTs/PCM composites was less than that of L-MWCNTs/PCM composites.

The quantitative results for DSC characteristics were obtained by analyzing DSC curves. By analyzing heating related part of DSC curve, melting onset temperature ( $T_{mo}$ ), melting peak temperature ( $T_{mp}$ ), melting endset temperature ( $T_{me}$ ) and melting latent heat ( $H_e$ ) are obtained. When similar analysis is performed for solidification-related part of DSC curve, solidification onset temperature ( $T_{so}$ ), solidification peak temperature ( $T_{sp}$ ), solidification endset temperature ( $T_{se}$ ) and solidification latent heat ( $H_s$ ) are obtained.

To run electronic equipments safely, phase change material (PCM) known as passive cooling system is an important alternative for the thermal protection. Due to their high fusion energy, PCMs are able to store large

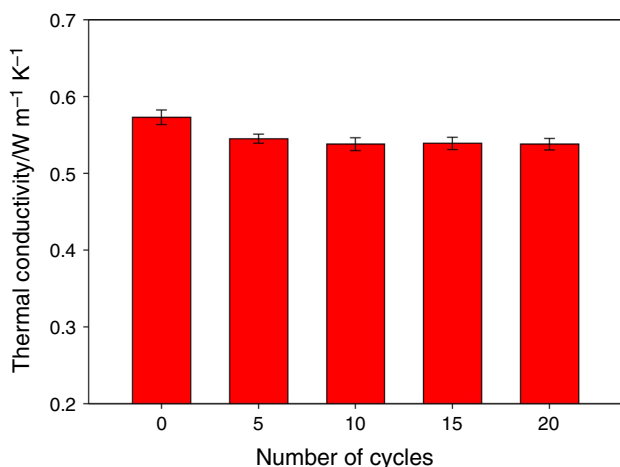


Fig. 4 Variation of thermal conductivity with respect to cycling

**Table 2** Thermal performances of the composites which have been obtained by being doped with single- and multi-walled carbon nanotubes

Reference	Nanoparticles	Mass fractions/ %	Maximum enhancement in thermal conduct. (device)	Variation of melting and solidification temperatures	Variation of melting and solidification latent heats
Present study	L-MWCNTs	1–5	43% (KD2 Pro)	MPT: none	MLH: decrease
	S-MWCNTs	1–5	18% (KD2 Pro)	SPT: increase	SLH: decrease
Zeng et al. [22]	MWCNT	1–5	30% (hot disk)	MPT: decrease SPT: nonmeasured	MLH: decrease SLH: nonmeasured
Zeng et al. [23]	MWCNT	1–5	26% (hot disk)	MPT: none SPT: none	MLH: decrease SLH: nonmeasured
Wang et al. [20]	MWCNT	1	46% (transient short hot wire)	MPT: decrease SPT: none	MLH: decrease SLH: none
Wang et al. [28]	MWCNT	0.2–1	51.6% (transient short hot wire)	MPT: none SPT: none	MLH: none SLH: none
Wang et al. [27]	MWCNT	0.2–2	40% (transient short hot wire)	MPT: decrease SPT: nonmeasured	MLH: decrease SLH: nonmeasured -
Teng et al. [29]	MWCNT	1–3	–	MPT: decrease SPT: increase	MLH: decrease SLH: decrease
Kumaresan et al. [21]	MWCNT	0.35–1.4	45% (KD2 Pro)	MPT: none SPT: none	MLH: decrease SLH: increase
Shaikh et al. [30]	MWCNT	0.1–1	–	MPT: nonmeasured	MLH: increase
	SWCNT			SPT: nonmeasured	SLH: nonmeasured
Cui et al. [31]	MWCNT	1–10	24%	MPT: none SPT: none	MLH: none SLH: none
Fan et al. [25]	MWCNT	1–5	30% (KD2 Pro)	MPT: decrease	MLH: decrease
				SPT: decrease	SLH: decrease
Yu et al. [26]	MWCNT	1–5	24% (KD2 Pro)	MPT: nonmeasured KNS: nonmeasured	MLH: nonmeasured SLH: nonmeasured

*MWCNT* multi-walled carbon nanotubes, *SMWCNT* single-walled carbon nanotubes, *L-MWCNTs* long multi-walled carbon nanotubes, *S-MWCNTs* short multi-walled carbon nanotubes, *MPT* melting point temperature, *SPT* solidification point temperature, *MLH* melting latent heat, *SLH* solidification latent heat

amount of energy compared to their light weight. They can be produced according to the required working temperature span to handle the thermal problem effectively. Most of the electronic equipments have a suitable operating temperature range of 233–358 K. Hence, to run electronic equipment safely, melting and solidification temperatures of PCMs should not deviate from the operating temperature limits. The melting and solidification temperatures of S-MWCNTs/PCM and L-MWCNTs/PCM composites have been given, respectively, in Tables 3 and 4. While  $T_{mo}$  and  $T_{mc}$  temperatures of PCM were measured, respectively, 343.23 and 386.07 K,  $T_{so}$  and  $T_{se}$  temperatures were measured, respectively, 375.28 and 340.78 K. As it can be seen, although melting phase change occurs in a wide temperature range of 42.84 K, solidification phase change occurs in a lower temperature range of 34.5 K. The exotherm peak of PCM shifted slightly to the left according to endotherm peak. This is the indicator of the degree of

supercooling. Supercooling degree is identified quantitatively as the difference between  $T_{mp}$  and  $T_{sp}$  [17] is determined as 1.79 K for PCM. On the other hand, the supercooling effect was measured in the range between 2 and 3 K for almost all composites doped with MWCNTs. When Tables 3 and 4 are examined, it was observed that except  $T_{so}$  and  $T_{se}$ , temperatures did not change depending on mass fraction and size of the MWCNTs. Furthermore,  $T_{so}$  temperature showed an increase up to 2.1% in comparison with PCM in case of being doped with MWCNTs. This case was considered that doped MWCNTs inside PCM increase nucleation effect. In contrast to this case,  $T_{se}$  slightly decreases for all composites studied, thereby causing an increase in solidification temperature range up to 7%.

The melting and solidification latent heats of PCM were measured as 227.67 and 217.09 J g<sup>-1</sup>, respectively. Notably, solidification latent heat resulted less than melting

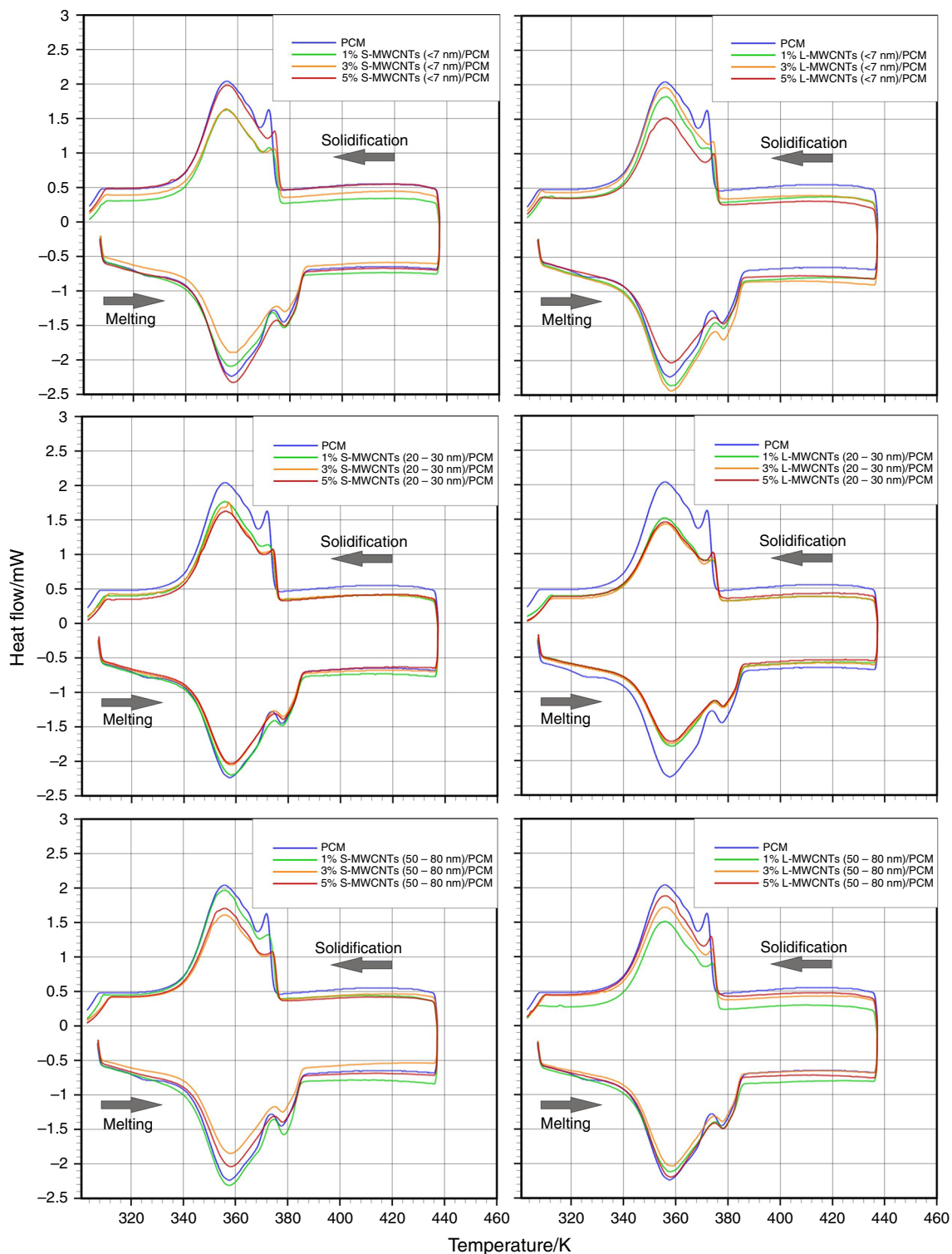


**Fig. 5** DSC curves of S-MWCNTs/and L-MWCNTs doped into PCM

latent heat because of incomplete crystallization during the solidification process [20]. The variation of melting and solidification latent heats of PCM composites doped with S-MWCNTs and L-MWCNTs as compared to MWCNTs

mass fraction doped is given in Fig. 6. The melting and solidification latent heats of PCMs doped with MWCNTs decrease depending on increase in mass fraction of MWCNTs. In fact, the most important reason for above-

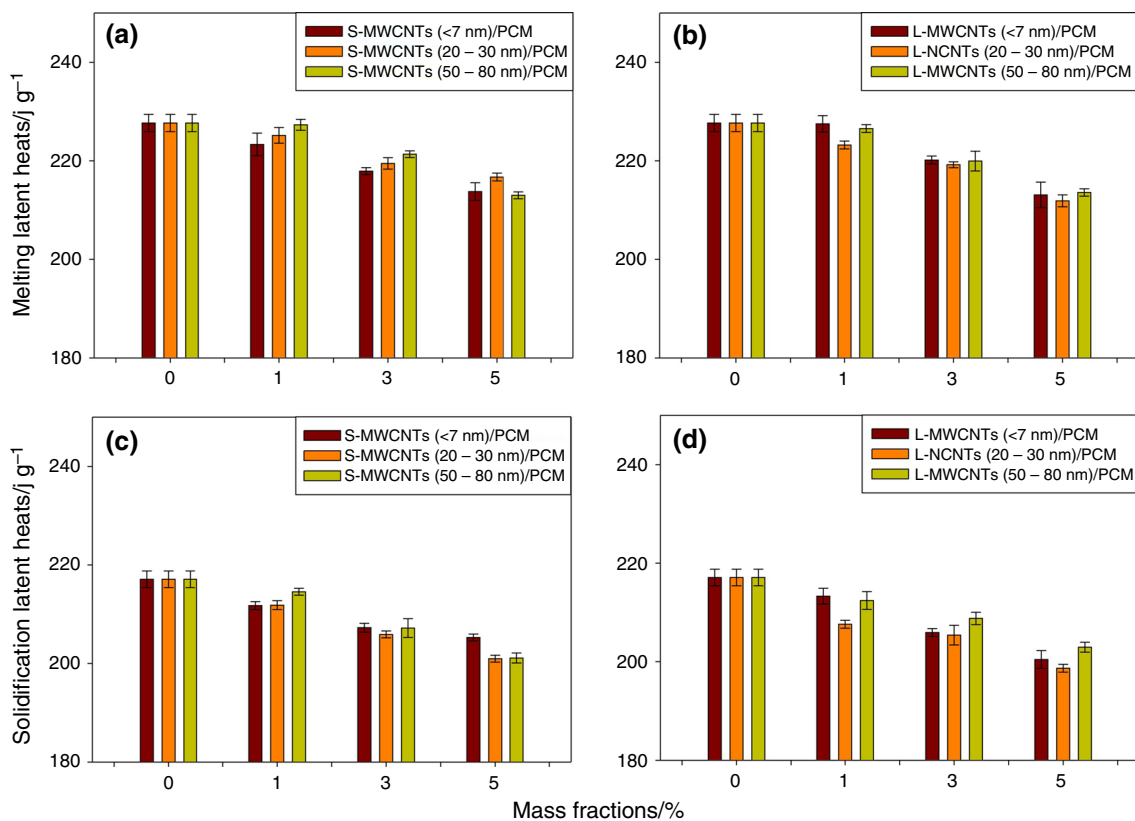


**Table 3** Melting and solidification temperatures of S-MWCNTs/PCM composites

Composite	PCM	S-MWCNTs (< 7 nm)			S-MWCNTs (20–30 nm)			S-MWCNTs (50–80 nm)		
		1%	3%	5%	1%	3%	5%	1%	3%	5%
Mass fract.	0%	1%	3%	5%	1%	3%	5%	1%	3%	5%
$T_{m0}/K$	343.22	342.87	342.98	343.74	343.67	343.27	343.52	342.48	342.93	343.30
$T_{mp}/K$	358.02	357.58	358.33	358.42	358.55	358.01	358.21	357.81	358.30	358.30
$T_{me}/K$	386.05	385.15	385.75	385.35	385.65	385.45	385.65	384.95	385.95	385.75
$T_{so}/K$	375.25	376.65	377.15	377.15	376.55	376.85	377.15	376.55	377.35	377.35
$T_{sp}/K$	356.23	355.55	355.64	356.15	355.88	356.36	356.08	355.76	355.96	355.76
$T_{se}/K$	340.78	339.89	340.01	339.56	339.71	339.01	339.36	340.10	339.76	339.79

**Table 4** Melting and solidification temperatures of L-MWCNTs/PCM composites

Composite	PCM	L-MWCNTs (< 7 nm)			L-MWCNTs (20–30 nm)			L-MWCNTs (50–80 nm)		
		1%	3%	5%	1%	3%	5%	1%	3%	5%
Mass fract.	0%	1%	3%	5%	1%	3%	5%	1%	3%	5%
$T_{m0}/K$	343.22	343.03	342.86	343.50	343.30	343.47	343.60	343.17	343.12	343.69
$T_{mp}/K$	358.02	358.66	358.39	358.32	358.23	358.04	358.10	358.15	358.24	358.37
$T_{me}/K$	386.05	385.45	385.85	385.55	386.05	385.65	385.55	385.65	385.35	385.05
$T_{so}/K$	375.25	376.55	377.25	377.35	377.45	377.45	377.35	377.15	376.95	376.65
$T_{sp}/K$	356.23	355.72	355.92	356.08	355.62	356.24	355.89	357.42	356.03	355.86
$T_{se}/K$	340.78	339.20	339.37	339.48	340.30	339.49	339.75	339.87	340.12	339.53

**Fig. 6** Variation of latent heats as a function of mass fractions a) melting latent heats of S-MWCNTs/PCM, b) melting latent heats of L-MWCNTs/PCM, c) solidification latent heats of S-MWCNTs/PCM, d) solidification latent heats of L-MWCNTs/PCM

mentioned phenomenon is that MWCNTs do not contribute to latent heats because phase change of MWCNTs does not occur in a temperature range of cooling to heating (303–433 K). It was considered that the decrease in latent heats to be proportional to the amount of PCM absorbed by MWCNTs. The diameter effect was seen only using S-MWCNTs especially at low mass fractions. When S-MWCNTs are used as filler, increase in diameter results less decrease in latent heats. It was considered that this situation is associated with more PCM absorbing nanoparticles with small diameter because of high surface area and dispersing capability. In contrast to this, S-MWCNTs with large diameter absorb less PCM because of its low surface area. When L-MWCNTs are used as filler, diameter effect disappears and variation of latent heats at each mass fraction shows the same behavior. However, at low mass fraction of L-MWCNTs, decrease in the latent heats was small because of less absorption of PCM by the MWCNTs. The reason for less absorption of PCM is agglomerating of the L-MWCNTs within the PCM matrix. In addition to this, PCM absorbing capability of the L-MWCNTs increased depending on the increase in mass fractions and so it results more decreasing in latent heat at higher mass fractions. As a result, it shows that diameter and lengths of MWCNTs doped inside PCM are effective on their energy storage capacities. Molecular interactions between surfaces of PCM and MWCNTs have been effective on energy storage capacities of composites [25].

## Conclusions

In this study, effects of the mass fraction and size of MWCNTs on thermal properties of MWCNTs/PCM composites were systematically investigated. It was found that the rate of increase in the value of thermal conductivity increases associated with increase in length and diameter of MWCNTs. Such that at 5% mass fraction, enhancement of thermal conductivities of PCM composites doped with S-MWCNTs and L-MWCNTs with the highest diameter size of 50–80 nm outer diameter was measured, respectively, 18.41 and 42.54%. In addition to this at 5% mass fraction, enhancement of thermal conductivity of PCM composites doped with L-MWCNTs with outer diameters of < 7 nm, 20–30 nm and 50–80 nm was measured as 9.95, 33.60 and 42.54%, respectively. On the other hand, it was determined that thermal conductivities of S-MWCNTs/PCM composites were less than those of PCM at the mass fraction of 1%. In addition to that, it was found that thermal conductivities of L-MWCNTs/PCM composites were almost the same with those of pure PCM at the same mass fraction. It was determined that while  $T_{mo}$ ,  $T_{mp}$  and  $T_{me}$  temperatures do not change depending on

mass fraction and size of MWCNTs doped,  $T_{so}$  and  $T_{se}$  temperatures change very little depending on MWCNTs mass fraction. Experimental findings obtained in this study showed that melting and solidification latent heats decreased for long and short MWCNTs depend on the increasing MWCNTs mass fraction. On the other hand, it was reported that the deterioration of the latent heats yielded 10% less than that of pure PCM in the highest mass fraction of 5%. It was concluded that using large diameter and long length of MWCNTs as a filler in PCMs will result in the highest enhancement in thermal conductivity with minimal change at melting/solidification temperatures.

**Acknowledgements** The authors gratefully acknowledge the financial support provided by ASELSAN INC.

## References

1. Sarier N, Onder E. Organic phase change materials and their textile applications: an overview. *Thermochim Acta*. 2012;540:7–60.
2. Fan LW, Khodadadi JM. Thermal conductivity enhancement of phase change materials for thermal energy storage: a review. *Renew Sustain Energy Rev*. 2011;15:24–6.
3. Oró E, de Garcia A, Castel A, Farid MM, Cabeza LF. Review on phase change materials (PCMs) for cold thermal storage applications. *Appl Energy*. 2012;99:513–33.
4. Zhou D, Zhao CY, Tian Y. Review on thermal energy storage with phase change material (PCMs) in building applications. *Appl Energy*. 2012;92:593–605.
5. Sahoo SK, Das MK, Rath P. Applications of TEC-PCM based heat sinks for cooling of electronic components: a review. *Renew Sustain Energy Rev*. 2016;59:550–82.
6. Li WQ, Qu ZQ, He YL, Tao YB. Experimental study of a passive thermal management system for high-powered lithium ion batteries using porous metal foam saturated with phase change materials. *J Power Sour*. 2014;255:9–15.
7. Weng YC, Cho HP, Chang CC, Chen SL. Heat pipe with PCM for electronic cooling. *Appl Energy*. 2011;88:1825–33.
8. Zhou G, He S. Thermal performance of a radiant floor heating system with different heat storage materials and heating pipes. *Appl Energy*. 2015;138:648–60.
9. Barzin R, Chen JJ, Young BR, Farid MM. Application of PCM energy storage in combination with ventilation for space cooling. *Appl Energy*. 2015;158:412–21.
10. Jin X, Shi D, Midina MA, Shi X, Zhou X, Zhang X. Optimal location of PCM layer in building walls under Nanjing (China) weather conditions. *J Therm Anal Calorim*. 2017;129:1767–78.
11. Ye WB. Enhanced latent heat thermal energy storage in the double tubes using fins. *J Therm Anal Calorim*. 2017;128:533–40.
12. Hadiya JP, Kumar A, Shukla N. Experimental thermal behaviour response of paraffin wax as storage unit. *J Therm Anal Calorim*. 2016;124:1511–8.
13. Sharma A, Tyagi VV, Chen CR, Buddhi D. Review on thermal energy storage with phase change materials and applications. *Renew Sustain Energy Rev*. 2009;13:318–45.
14. Yuan Y, Li T, Zhang N, Cao X, Yang X. Investigation on thermal properties of capric–palmitic–stearic acid/activated carbon composite phase change materials for high-temperature cooling application. *J Therm Anal Calorim*. 2016;124:881–8.

15. Strith U. An experimental study of enhanced heat transfer in rectangular PCM thermal storage. *Int J Heat Mass Transf.* 2004;47:2841–7.
16. Agyenim F, Eames P, Smyth M. A comparison of heat transfer enhancement in a medium temperature thermal energy storage heat exchanger using fins. *Sol Energy.* 2009;83:1509–20.
17. Zhang P, Mang Z, Zhu H, Yanling W, Peng S. Experimental and numerical study of heat transfer characteristics of a Paraffin/metal foam composite PCM. *Energy Proc.* 2015;75:3091–7.
18. Xiao M, Feng B, Gong KC. Preparation and performance of shape stabilized phase change thermal storage materials with high thermal conductivity. *Energy Convers Manag.* 2002;43:103–8.
19. Yang J, Yang L, Xu C, Du X. Experimental study on enhancement of thermal energy storage with phase change material. *Appl Energy.* 2016;169:164–76.
20. Wang J, Xie H, Xin Z, Li Z, Li Y, Chen L. Enhancing thermal conductivity of palmitic acid based phase change materials with carbon nanotubes as fillers. *Sol Energy.* 2010;84:339–44.
21. Kumerasan V, Velraj R, Das SK. The effect of carbon nanotubes in enhancing the thermal transport properties of PCM during solidification. *Heat Mass Transf.* 2012;48:1345–55.
22. Zeng JL, Liu YY, Cao ZX, Zhang J, Zhang ZH, Sun LX, Xu F. Thermal conductivity enhancement of MWCNTs on the pentaerythritol tetradecanoate form-stable PCM. *J Therm Anal Calorim.* 2008;91:443–6.
23. Zeng JL, Cao Z, Yang DW, Xu F, Sun LX, Zhang XF, Zhang L. Effects of MWCNTs on phase change enthalpy and thermal conductivity of a solid–liquid organic PCM. *J Therm Anal Calorim.* 2009;95:507–12.
24. Wu SY, Tang X, Nie CD, Peng DQ, Gong SG, Wang ZQ. The effects of various carbon nanofillers on the thermal properties of paraffin for energy storage applications. *J Therm Anal Calorim.* 2016;124:181–8.
25. Fan LW, Fang X, Wang X, Zeng Y, Xiao YQ, Yu ZT, Xu X, Hu YC, Cen KF. Effects of various carbon nanofillers on the thermal conductivity and energy storage properties of paraffin-based nanocomposite phase change materials. *Appl Energy.* 2013;110:163–72.
26. Yu ZT, Fang X, Fan LW, Wang X, Xiao YQ, Zeng Y, Xu X, Hu YC, Cen KF. Increased thermal conductivity of liquid paraffin-based suspensions in the presence of carbon nano-additives of various sizes and shapes. *Carbon.* 2013;53:277–85.
27. Wang J, Xie H, Xin Z. Thermal properties of paraffin based composites containing multi-walled carbon nanotubes. *Thermochim Acta.* 2009;488:39–42.
28. Wang J, Xie H, Xin Z, Li Y. Increasing the thermal conductivity of palmitic acid by the addition of carbon nanotubes. *Carbon.* 2010;48:3979–86.
29. Teng TP, Yu CC. The effect on heating rate for phase change materials containing MWCNTs. *Int J Chem Eng Appl.* 2012;3:340–2.
30. Shaikh S, Lafdi K, Hallinan K. Carbon nanoadditives to enhance latent energy storage of phase change materials. *J Appl Phys.* 2008;103:094302.
31. Cui Y, Liu C, Hu S, Yu X. The experimental exploration of carbon nanofiber and carbon nanotube additives on thermal behaviour of phase change materials. *Sol Energy Mater Sol Cells.* 2011;95:1208–12.
32. Huxtable ST, Cahill DG, Shenogin S, Xue LP, Ozisik R, Barone P, Usrey MS, Siddons G, Shim M, Kebliski P. Interfacial heat flow in carbon nanotube suspension. *Nat Mater.* 2003;2:731–4.
33. Chen YJ, Nguyen DD, Shen MY, Yip MC, Tai NH. Thermal characterization of the graphite nanosheets reinforced paraffin phase change composites. *Compos A.* 2013;44:40–6.
34. Sharma RK, Ganesan P, Tyagi VV. Long-term thermal and chemical reliability study of different organic phase change materials for thermal energy storage applications. *J Therm Anal Calorim.* 2016;124:1357–66.